HHS Public Access

Author manuscript

Nat Immunol. Author manuscript; available in PMC 2016 August 22.

Published in final edited form as:

Nat Immunol. 2016 April ; 17(4): 433–440. doi:10.1038/ni.3385.

The microRNA miR-148a functions as a critical regulator of B cell tolerance and autoimmunity

Alicia Gonzalez-Martin[1], **Brian D Adams**[2], **Maoyi Lai**[1], **Jovan Shepherd**[1], **Maria Salvador-Bernaldez**[3], **Jesus M Salvador**[3], **Jun Lu**[2], **David Nemazee**[1], and **Changchun Xiao**[1,*]

[1]Department of Immunology and Microbial Science, The Scripps Research Institute, La Jolla, CA 92037, USA

[2]Department of Genetics, Yale Stem Cell Center, Yale Cancer Center, and Yale Center for RNA Science and Medicine, Yale University, New Haven, CT 06520, USA

[3]Department of Immunology and Oncology, National Biotechnology Center, Madrid, Spain

SUMMARY

Autoreactive B cells play critical roles in a large diversity of autoimmune diseases, but the molecular pathways controlling these cells remain poorly understood. We performed an *in vivo* functional screen of a lymphocyte-expressed miRNA library and identified the microRNA miR-148a as a potent regulator of B cell tolerance. Elevated miR-148a expression impaired B cell tolerance by promoting the survival of immature B cells upon B cell receptor engagement via suppressing the expression of *Gadd45a*, *Pten* and *Bcl2l11*, which encodes the pro-apoptotic factor Bim. Furthermore, increased expression of miR-148a, which occurs frequently in lupus patients and lupus-prone mice, facilitated the development of lethal autoimmune disease in a lupus mouse model. These studies demonstrate that miR-148a functions as an important regulator of B cell tolerance and autoimmunity.

INTRODUCTION

Immune tolerance ensures that the pool of lymphocytes present in an individual's immune system can react to a vast variety of foreign antigens but do not attack the self-tissues. Defects in immune tolerance mechanisms constitute the basis for the development of autoimmunity that is characterized by tissue damage caused by self-reactive lymphocytes. Autoreactive B cells play critical roles in a broad spectrum of human autoimmune diseases

Correspondence should be addressed to C.X. (; Email: cxiao@scripps.edu) **or D.N**. (; Email: nemazee@scripps.edu)

AUTHOR CONTRIBUTIONS

C.X., D.N. and A.G.M. conceptualized and designed the project. A.G.M. performed most of the experiments. B.D.A. and J.L. provided the retroviral miRNA-expression library for pool screening and retroviral vectors encoding individual miRNAs for positive hit validation, and performed miRNA barcode analysis to identify miRNAs that broke B cell tolerance. M.L. performed bone marrow reconstitution experiments with Bim- and PTEN-deficient mice. M.S.B. and J.M.S. bred Gadd45a-deficient mice, harvested bones and shipped to A.G.M. for bone marrow reconstitution experiments. J.S. managed the mouse colony and provided technical support. C.X. and D.N. supervised the project. A.G.M., C.X. and D.N. wrote the manuscript with contribution from all authors.

COMPETING FINANCIAL INTERESTS

The authors declare no competing financial interests.

such as systemic lupus erythematosus, rheumatoid arthritis, diabetes and multiple sclerosis by producing autoantibodies, presenting autoantigens to T cells, and secreting proinflammatory cytokines[1].

B cell tolerance initiates in the bone marrow at the immature stage of B cell development by a series of mechanisms known as central tolerance. Immature B cells, which express their first functional B cell antigen receptor (BCR), a membrane-bound immunoglobulin M (IgM), arise as the result of successful rearrangements at the genes encoding immunoglobulin heavy (IgH) and light (IgL) chains. The combinatorial and stochastic nature of these rearrangements ensures diversity in the BCR repertoire but also generates B cells that recognize self-antigens. To remove these potentially harmful autoreactive B cells, immature B cells undergo the first immune tolerance checkpoint. If the newly generated immature B cell is non-autoreactive, it exits the bone marrow and matures in the periphery. If the immature B cell recognizes self-antigens, it continues to rearrange the light chain to generate a non-autoreactive IgM through receptor editing. If receptor editing is unsuccessful, the autoreactive B cell then dies by apoptosis (clonal deletion). Since not all peripheral self-antigens are adequately expressed in the bone marrow, additional B cell tolerance checkpoints exist in the periphery[2, 3]. Previous studies showed that autoreactivity is progressively diminished during normal B cell development, suggesting that multiple B cell tolerance mechanisms regulate autoreactive B cells[4, 5]. It has been shown that both central and peripheral B cell tolerance mechanisms are defective in human autoimmune diseases including lupus, rheumatoid arthritis and multiple sclerosis[6, 7, 8].

Despite intensive study, the molecular mechanisms underlying B cell tolerance are poorly understood. Specifically, the role of individual microRNAs (miRNAs) in B cell tolerance remains unexplored. MiRNAs are 19–23 nucleotides long endogenously encoded small RNAs that regulate the expression of its target genes by pairing through imperfect sequence complementarity with its target messenger RNAs (mRNAs) and promoting mRNA degradation and/or translational repression[9]. Hundreds of miRNAs are expressed in the immune system and they play essential roles in regulating lymphocyte development and function[10, 11, 12, 13]. Expression profiling studies revealed that many miRNAs are dysregulated in lymphocytes from patients with autoimmune diseases[14, 15, 16, 17], and mouse genetic studies have established causative roles for a few of those miRNAs in regulating autoimmunity through T cells[18, 19, 20, 21, 22, 2324, 25, 26, 27, 28]. However, no study to our knowledge has addressed the potential contribution of individual miRNAs to the regulation of autoreactive B cells.

We performed a functional screen using a retroviral miRNA-expression library and the recently established IgM^b-macroself mouse model of B cell tolerance[29, 30]. In this model, mice ubiquitously express an engineered membrane-bound superantigen reactive to the constant region of IgM. These mice present normal early B cell development, which results in an unaltered immature B cell repertoire. Once B cells reach the immature B cell stage, their membrane-bound IgM recognizes the superantigen, which mimics self-antigen recognition. In this context, receptor editing is ineffective in eliminating superantigen reactivity, and all developing B cells die by clonal deletion, resulting in a nearly complete absence of mature B cells in the spleen and lymph nodes[30]. We took a retroviral transduction

and bone marrow reconstitution approach in which bone marrow stem and precursor cells (HSPCs) from compatible mice were transduced with retroviruses encoding a miRNA-expression library, and used to reconstitute irradiated IgM^b-macroself recipient mice. This system provides a clean readout for the identification of miRNAs that control B cell tolerance: if B cells are present in the spleen of those mice after reconstitution, escape from B cell tolerance has occurred and the miRNAs over-expressed by these splenic B cells can then be identified[29]. In the present study, we identified miR-148a as a critical regulator of B cell tolerance and autoimmunity.

RESULTS

miR-148a regulates B cell tolerance

To identify miRNAs that regulate B cell tolerance, we performed an *in vivo* functional screen of a retroviral library of 113 lymphocyte-expressed miRNAs, which were divided into four pools (Pools 1 to 4) containing 20–37 miRNAs in each pool (Table 1). The relatively small pool size was determined based on recent studies showing that only 30–50 unique HSPC clones can be successfully engrafted in bone marrow reconstitution experiments[29, 31]. The virus mixtures were used to transduce HSPCs obtained from the bone marrow of donor C57BL/6J mice that had been previously inoculated with 5-fluorouracil (5-FU) four days before. The transduced cells were transferred into irradiated recipient IgM^b-macroself mice to reconstitute their immune system. Eight weeks after reconstitution, mice were euthanized and the presence of B cells (CD19$^+$IgM$^+$) in the spleen was analyzed. The IgM^b-macroself mice that received HSPCs transduced with the control virus, which does not encode any miRNA, had virtually no B cells in the spleen (Fig. 1a). Recipient mice that received cells transduced with pool 2 retroviruses showed significant escape from B cell tolerance, as indicated by the presence of a clear CD19$^+$IgM$^+$ B cell population in the spleen (Fig. 1a–c). Other retrovirus pools showed marginal effects, if any. Therefore, we focused on pool 2 for the identification of miRNAs that are able to break B cell tolerance.

We used unique sequences (referred to as barcodes hereafter) present in the regions flanking the miRNA hairpin of each of the miRNA constructs of our library (Supplementary Fig. 1a–c) to identify miRNAs that led to the loss of B cell tolerance[29]. B lymphocytes (CD19$^+$ cells) from the spleens of pool 2-transduced IgM^b-macroself mice were purified, and their genomic DNA was extracted and submitted to barcode analysis. Since we started from a pool of retroviruses whose individual members might have different capacity to infect or to affect the survival and proliferation of HSPCs, we also purified CD19$^+$IgM$^-$ B cell precursors from the bone marrow of the same mice and used their genomic DNA as internal controls. MiRNAs driving the break of B cell tolerance should be enriched in spleen B cells when compared with bone marrow B cell precursors from the same mouse, because the precursor cells have not yet been subjected to selection imposed by the IgM^b-macroself superantigen, while spleen B cells represent post-selection cells. Barcode analysis revealed seven miRNAs, miR-511, miR-148a, miR-26a, miR-26b, miR-342, miR-423 and miR-182, that exhibited more than 4-fold enrichment in splenic B cells (Fig. 2a,b).

To validate the positive hits, retroviruses encoding each candidate miRNA were used to transduce donor bone marrow cells from C57BL/6J mice following the same experimental

approach as for the pooled screening experiments. Among the 7 candidate miRNAs, miR-148a showed the most significant break of B cell tolerance, with an average of approximately 16% B cells of total splenocytes (Fig. 2c–e). miR-26a, miR-26b, miR-342, miR-423 and miR-182 showed a more limited loss of tolerance, with average splenic B cell percentages ranging from 5% to 8%. Retroviral expression of miR-511 did not rescue B cells from deletion in IgM^b-macroself mice, with splenic B cell percentages close to mice reconstituted with control virus-transduced cells which showed approximately 2% B cells of total splenocytes (Fig. 2c–e). We also reconstituted IgM^b-macroself mice with HSPCs co-infected with a mixture of retroviruses encoding six miRNAs identified in our screen (miR-148a, -26a, -26b, -342, -423 and -511). Analysis of those mice failed to reveal synergistic effects between these miRNAs in the regulation of B cell tolerance (Supplementary Fig. 2a–c). These results indicate that the IgM^b-macroself model is a robust *in vivo* system for the identification of miRNAs that regulate B cell central tolerance, and demonstrate that miR-148a is a potent regulator of this process.

miR-148a protects immature B cells from apoptosis

Previous miRNA profiling studies showed that miR-148a expression is tightly regulated throughout B cell development[10]. miR-148a is highly expressed in pro- and pre-B cells, substantially downregulated upon differentiation into immature and mature B cells, and induced upon B cell activation and differentiation into germinal center B cells (Supplementary Fig. 3a)[10]. Interestingly, BCR engagement only modestly increased miR-148a expression in B cells when compared with stimulation using lipopolysaccharide (LPS), and diminished LPS-induced miR-148a expression when the two stimuli were used together (Supplementary Fig. 3b). Upregulation of miR-148a expression occurs frequently in autoimmune diseases. Increased miR-148a abundance was found in B cells, T cells, and tissue lesions of human patients with systemic lupus erythematosus, rheumatoid arthritis, and multiple sclerosis[14, 15, 16, 17, 32], as well as in splenic lymphocytes of NZB/W mice at the age of 3–4 months, when overt disease has not yet become evident in this lupus mouse model[18, 33]. We hypothesize that, under physiological conditions, low amounts of miR-148a in immature B cells render autoreactive cells sensitive to apoptosis induced by BCR engagement during central B cell tolerance. In humans and mice predisposed to autoimmune diseases, elevated miR-148a expression makes immature B cells resistant to BCR-induced apoptosis and this leads to the escape of autoreactive B cells from clonal deletion. These autoreactive B cells would then contribute to the development of autoimmune diseases in those individuals.

We tested this hypothesis in the WEHI-231 immature B cell line, an *in vitro* model of B cell clonal deletion. These cells arrest at G_1 in the cell cycle upon culture with cross-linking IgM-specific antibodies and subsequently die by apoptosis[34, 35]. Thus, stimulation of WEHI-231 cells with anti-IgM is a widely used method to mimic the recognition of a self-antigen by immature B cells as it would occur during the central tolerance checkpoint. Similar to murine immature B cells, these cells express low endogenous amounts of miR-148a (Fig. 3a and Supplementary Fig. 3a). To investigate the effect of elevated miR-148a expression on WEHI-231 cells, these cells were transduced with control or miR-148a-expressing retroviruses that also encode green fluorescent protein (GFP), and

sorted to purify transduced cells and generate the stable cell lines WEHI-control and WEHI-miR-148a. The resulting WEHI-miR-148a cells showed robust miR-148a expression when compared with WEHI-control cells (Fig. 3a). We stimulated these cell lines with anti-IgM and examined their growth and survival. Consistent with previous reports, anti-IgM stimulation of WEHI-control cells led to a severe slowdown in their growth (Fig. 3b). In contrast, WEHI-miR-148a cells exhibited only a transient retardation in growth in response to anti-IgM stimulation and recovered by 72 h (Fig. 3b). Examination of cell apoptosis by annexin V and active caspase 3 staining showed that a significant fraction of WEHI-control cells underwent apoptosis in response to anti-IgM stimulation, while WEHI-miR-148a cells were largely resistant to anti-IgM-induced apoptosis (Fig. 3c–f). The proliferation of WEHI-control and WEHI-miR-148a cells was examined by labeling them with the fluorescent dye cell trace violet (CTV). When gated on live cells, CTV dilution over time was comparable between WEHI-control and WEHI-miR-148a cells (Fig. 3g), suggesting that miR-148a does not affect proliferation. Therefore, miR-148a controls B cell central tolerance by regulating the apoptosis of immature B cells upon BCR engagement.

miR-148a targets Gadd45a, Bim, and PTEN

To gain insight into the molecular mechanisms through which miR-148a regulates BCR engagement-induced apoptosis in immature B cells, we performed RNA-sequencing analysis of WEHI-control and WEHI-miR-148a cells in the presence of anti-IgM stimulation. Since elevated miRNA expression promotes the degradation of its target gene mRNAs, miR-148a target gene mRNA abundance should be lower in WEHI-miR-148a than in WEHI-control cells. We identified 119 protein-coding genes that showed at least 1.5-fold reduction in their mRNA abundance in WEHI-miR-148a and contained predicted miR-148a binding sites (Supplementary Table 1). Among those, targets previously implicated in cell survival were of special interest because our results suggested a role for miR-148a in protecting immature B cells from BCR-induced apoptosis. This resulted in the selection of four target genes, *Bcl2l11* (encoding Bim), *Tnfrsf1b* (encoding tumor necrosis factor receptor 2, TNFR2), *Pten* and *Gadd45a*, which presented 2.4-, 2.3-, 1.8- and 1.5-fold reduction by miR-148a respectively, for further study.

The RNA-sequencing results were validated by qRT-PCR, and the protein expression encoded by these genes was examined by immunoblot (Bim and PTEN) or flow cytometry (TNFR2). Murine Gadd45a protein expression was not measured due to the lack of a suitable antibody. *Bcl2l11*, *Pten* and *Gadd45a* exhibited miRNA148a-mediated reduction in their mRNAs (Fig. 4a). Bim and PTEN protein abundance as well as cell surface expression of TNFR2 were also reduced by elevated miR-148a expression (Fig. 4b and Supplementary Fig. 4a). We also measured the protein and mRNA expression of Gadd45a, Bim, Tnfr2 and PTEN in two other WEHI-231 stable cell lines that expressed different miRNAs (miR-26a and miR-182). miR-26a decreased the expression of Bim and PTEN but not Gadd45a and Tnfr2, while miR-182 did not affect the expression of any of the targets analyzed (Supplementary Fig. 4a and Supplementary Fig. 5a,b).

To demonstrate direct regulation of *Bcl2l11*, *Pten* and *Gadd45a* by miR-148a we performed dual-luciferase reporter assays. Gene fragments encoding 3’UTR regions of these targets

were cloned into the expression vector psiCHECK2, which encodes the renilla luciferase controlled by the cloned 3'UTR (Supplementary Table 2). These constructs were co-transfected in HEK293 cells with an expression vector encoding miR-148a and the regulation of protein expression by miR-148a was measured. miR-148a significantly reduced reporter protein expression through the 3'UTR regions of *Bcl2l11*, *Pten* and *Gadd45a* (Fig. 4c). When the binding sites for miR-148a were mutated, this reduction was abolished. Therefore, miR-148a can suppress the expression of Bim, PTEN and Gadd45a protein through its cognate binding sites in 3'UTR of their respective transcript.

Gadd45a, Bim and PTEN regulate B cell central tolerance

We next investigated whether downregulation of these miR-148a target genes can break B cell tolerance. We obtained germline-deficient mice for *Gadd45a*, *Bcl2l11* and *Tnfrsf1b*, and generated *Cd19*-Cre *Pten*$^{fl/+}$ and *Cd19*-Cre *Pten*$^{fl/fl}$ mice[36, 37, 38, 39, 40]. Bone marrow cells from these mice were used to reconstitute lethally irradiated IgM^{b}-macroself mice, which were analyzed eight weeks later. The presence of splenic B cells in recipient mice would indicate that downregulation or complete loss of expression of the corresponding target gene is sufficient to impair B cell central tolerance, and that this target gene is an important regulator of this process.

When we used *Gadd45a*$^{-/-}$ mice as bone marrow donors to reconstitute lethally irradiated IgM^{b}-macroself mice, a very robust break of B cell tolerance was observed (Fig. 5a–c). The B cell percentage and total number in the spleen were higher than those caused by retroviral miR-148a expression. It is thought that miRNAs exert their functions by downregulating the expression of their target genes, not by a complete shutoff of their expression. For this reason we performed the same bone marrow reconstitution experiment using *Gadd45a*$^{+/-}$ mice as bone marrow donors. In this case, a reduction in *Gadd45a* expression was sufficient for a substantial number of B cells to escape the central tolerance checkpoint (Fig. 5a–c). These results reveal a previously unknown role of Gadd45a in regulating B cell central tolerance.

Previous studies have shown that Bim and PTEN regulate B cell central tolerance. A complete loss of Bim led to the accumulation of hen egg lysozyme (HEL)-binding B cells in the spleen of double transgenic mice with B cell specific expression of anti-HEL BCR (Ig HEL) and ubiquitous expression of a membrane-bound form of the HEL protein (mHEL)[41]. Similarly, a complete loss of PTEN improved the viability of immature B cells upon BCR crosslinking by anti-IgM in cell culture experiments[42]. We reconstituted lethally irradiated IgM^{b}-macroself mice with bone marrow cells from *Bcl2l11*$^{+/-}$, *Bcl2l11*$^{-/-}$, *Cd19*-Cre *Pten*$^{fl/+}$, and *Cd19*-Cre *Pten*$^{fl/fl}$ mice. Heterozygous deletion of *Bcl2l11* restored B cell development in IgM^{b}-macroself mice to a degree similar to that caused by retroviral miR-148a expression, and a complete loss of *Bcl2l11* led to B cell accumulation to a percentage and number almost identical to that found in wild-type C57BL/6J mice, which is typically around 55±1.4% and 47±4.4 ×10^{6} B cells (Fig. 5d–f). While heterozygous deletion of *Pten* led to the escape of tolerance by only a relatively small number of B cells, homozygous deletion caused the accumulation of more B cells in the spleen than found in wild-type C57BL/6J mice (Fig. 5g–i). The effect of reduced TNFR2 protein expression was

also examined. A complete deletion of *Tnfrsf1b* resulted in the accumulation of only a small number of B cells in the spleen of IgM^b-macroself mice (Supplementary Fig. 4b–d). These results demonstrate that Gadd45a, Bim and PTEN are dose-sensitive regulators of B cell central tolerance.

miR-148a accelerates the development of autoimmunity

Previous studies showed that miR-148a is upregulated in lymphocytes from lupus patients and mouse model of lupus[14, 15, 16, 17, 18, 32, 33]. In the latter, miR-148a upregulation was found before disease onset[18, 33]. Those findings suggest that miR-148a upregulation contributes to the development of lupus, instead of being a consequence of the disease. We next investigated the functional relevance of miR-148a upregulation in the development of autoimmune disease in MRL-lpr mice, a commonly used model for lupus research[43]. Consistent with previous reports, B cells from 6-week-old MRL-lpr mice were not activated in the periphery, but showed a 3-fold increase in miR-148a expression when compared to C57BL/6J control mice (Supplementary Fig. 6a,b). HSPCs from MRL-lpr mice were transduced with control or miR-148a-expressing retroviruses and used to reconstitute lethally irradiated MRL-lpr mice, which were monitored for the development of autoimmune disease. MLR-lpr mice reconstituted with miR-148a-expressing HSPCs showed disease symptoms significantly earlier than the control group. Once sick, the disease also progressed faster in the miR-148a group, eventually leading to a shorter life span for all mice in this group (Fig. 6a). miR-148a expression was measured in splenic B cells from these mice. The miR-148a group showed a 5–9-fold increase when compared to the control group reconstituted with vector-transduced MRL-lpr cells (Supplementary Fig. 6c), which is comparable to the increased levels found in lymphocytes from lupus patients[14, 15, 16, 17]. Serum samples were collected at different time points and examined for the presence of anti-double stranded-DNA (dsDNA) autoantibodies, a hallmark of lupus pathogenesis[43]. At 8 weeks after reconstitution low titers of dsDNA autoantibodies were detected in both groups at similar concentrations. From week 14 and on, mice in both groups showed increased concentrations of anti-dsDNA autoantibodies, but on average the miR-148a group had more anti-dsDNA autoantibodies than the control group, though the difference did not reach statistical significance due to individual variations (Fig. 6b). The secondary lymphoid organs were collected at terminal analysis, weighed and the cell number was determined. The peripheral lymph nodes (pLN) of mice in the miR-148a group were much bigger and contained significantly more cells than those in the control group, despite their shorter lifespan (Fig. 6c,d). No significant differences in weight and cellularity were found for the spleen and mesenteric lymph nodes (mLNs). Flow cytometry analysis revealed a substantial expansion of B cells in both the spleen and peripheral lymph nodes (pLNs) in the miR-148a group mice (Fig. 6e,f). These results demonstrate the functional importance of miR-148a upregulation in autoimmune disease.

DISCUSSION

Expression profiling studies have shown that miRNA dysregulation occurs frequently in lymphocytes from human patients with autoimmune diseases[44]. In the present study, we performed an *in vivo* functional screen of a miRNA library in the IgM^b-macroself model and

identified miR-148a as a critical regulator of B cell central tolerance and autoimmunity. miR-148a protects immature B cells from apoptosis induced by BCR engagement by suppressing the expression of *Gadd45a*, *Bcl2l11*, and *Pten*. Moreover, increased miR-148a expression accelerated the development of lethal autoimmune disease in MRL-lpr mice. These studies establish miR-148a as a potent regulator of B cell tolerance and, when dysregulated, as an important driver of autoimmune disease.

A miRNA often interacts with mRNAs of hundreds of target genes[9]. However, it has been thought that only a small number of key target genes mediate its function. The functions of these key targets are often sensitive to the cellular concentrations of their proteins[13]. By performing RNA-sequencing analysis of WEHI-231 cells, an immature B cell line, that overexpress miR-148a, we identified 119 protein coding genes whose expression is downregulated by miR-148a and contain miR-148a binding sites in their mRNAs. Because elevated miR-148a expression protected WEHI-231 cells from apoptosis induced by BCR engagement, we focused on target genes previously implicated in regulating cell survival. Further analysis identified *Gadd45a*, *Bcl2l11*, and *Pten* as functional target genes of miR-148a, as their expression was suppressed by miR-148a and their heterozygous deletion mimicked miR-148a-mediated break of B cell tolerance in the IgM^b-macroself model.

Bim and PTEN proteins have been previously shown to play important roles in regulating B cell tolerance and preventing autoimmunity. Both $Bcl2l11^{+/-}$ and $Pten^{+/-}$ mice developed lethal autoimmunity[36, 45]. A complete loss of Bim expression renders immature B cells resistant to BCR-induced apoptosis, breaks B cell central tolerance, and impairs B cell anergy in the periphery[41, 46]. Similarly, ablation of the *Pten* gene protects immature B cells from BCR-induced cell death and impairs B cell anergy[42, 47]. Those findings are consistent with the protective role that miR-148a plays in WEHI-231 cells. Both WEHI-231 cells and murine immature B cells express low amounts of miR-148a, which may be essential for maintaining their sensitivity to apoptosis induced by BCR engagement.

Our study uncovers a previously unknown role for Gadd45a in regulating B cell tolerance. Gadd45a is a ubiquitously expressed protein that is often induced by DNA damage and other stress signals associated with growth arrest and apoptosis[48]. Gadd45a-deficient mice developed a lupus-like autoimmune disease, characterized by high titers of autoantibodies, lymphoproliferation, autoimmune glomerulonephritis and premature death[40]. Gadd45a was found to prevent autoimmunity by functioning as a natural inhibitor of spontaneous p38 activation in T cells[49]. In this study, we show that Gadd45a also functions as dose-sensitive regulator of B cell tolerance. Both heterozygous and homozygous deletion of *Gadd45a* allows the escape of autoreactive B cells from the central tolerance checkpoint, which should contribute to the lethal autoimmune disease developed in $Gadd45a^{-/-}$ mice.

Interestingly, a link has been established between Gadd45a expression and Bim function. The Bim isoforms BimL and BimEL are normally found associated with motor complexes bound to dynein and sequestered in the cytoskeleton. Bim-induced apoptosis involves the release of BimL and BimEL from these microtubule-associated complexes and their translocation to mitochondria. A previous study reported that inducible expression of Gadd45a causes dissociation of Bim from microtubule associated components and its

translocation to mitochondria where it accumulates and triggers the apoptotic pathway[50]. This suggests functional cooperation between the miR-148a targets *Bcl2l11* and *Gadd45a* to regulate the apoptosis machinery required for the deletion of autoreactive immature cells during B cell central tolerance.

Intriguingly, all the three miR-148a target genes identified in this study as critical mediators of B cell central tolerance, *Gadd45a*, *Bcl2l11* and *Pten*, were previously implicated in autoimmunity, as mice with homozygous deletion of *Gadd45a* and mice with heterozygous deletion of *Pten* or *Bcl2l11* developed systemic autoimmune diseases resembling human lupus. Upregulation of miR-148a occurs frequently in both B and T cells of patients with systemic lupus erythematosus and rheumatoid arthritis, as well as in splenic lymphocytes of NZB/W lupus-prone mice even before disease onset[14, 15, 16, 17, 18, 32, 33], but whether this upregulation has any functional relevance in these diseases remained unknown. We investigated this in MRL-lpr mice, and showed that increased expression of miR-148a significantly accelerated the development of lethal autoimmune disease in these mice, thereby establishing a causative relationship between miR-148a upregulation and autoimmune disease.

In summary, this study demonstrates that IgM^b-macroself is a robust model for performing *in vivo* functional screens to identify novel regulators of B cell central tolerance, and that miRNA target gene identification and validation is an effective way to discover new protein coding genes regulating immune tolerance. We identified miR-148a as a critical regulator of B cell tolerance and autoimmunity, and uncovered a previously unknown role for Gadd45a in regulating B cell central tolerance. These insights into the mechanisms that control self-tolerance may lead to new strategies for the treatment of autoimmunity.

METHODS

Mice

The generation of IgM^b-macroself (MMRRC Strain 36510), *Gadd45a*$^{-/-}$, *Bcl2l11*$^{-/-}$, *Pten*$^{fl/fl}$ (Jax stock 006440), *Cd19*-Cre (Jax stock 006785), *Tnfrsf1b*$^{-/-}$ mice (Jax stock 002620), and MRL-lpr (Jax stock 000485) was previously reported[30, 36, 37, 38, 39, 40]. All mice were bred and housed under SPF conditions. All animal experiments were approved by Animal Care and Use Committee of The Scripps Research Institute and Ethics Committee of the Spanish National Biotechnology Center.

Retrovirus production

Retroviruses were generated by cotransfection of HEK293T cells with the pMIRWAY library (which contain GFP as a reporter gene), GAG-POL, and VSV-G plasmid[29]. For pooled screening, retroviral vectors encoding lymphocyte-expressed miRNAs were divided into 4 pools and used for virus generation. For positive hit validation, individual retroviral vectors encoding relevant miRNAs from the pMIRWAY library were used for retrovirus production. Confluent HEK293T cells were plated at a dilution 1:5 the day before transfection. Cells were co-transfected with miRNA pools or individual members, along with packaging plasmids. Cell culture media was replaced at 24 h post-transfection. At 48 h

post-transfection, virus containing-supernatant was collected, filtered, aliquoted, and stored at −80°C until use. The virus titer was determined by serial dilution of the viral supernatant and analysis of GFP positivity among infected target cells.

In vivo functional screen of miRNAs

Donor C57BL/6J mice were injected with 5-fluorouracil (Sigma) at a concentration of 150 mg/kg. Four days later bone marrow cells were isolated and HSPCs were enriched by Ficoll (GE Healthcare) density gradient centrifugation. Cells were resuspended in X-vivo 15 medium (Lonza) supplemented with 10% BSA, 2 mmol/l L-Glutamine and Pen/Strep, 100 μM 2-mercaptoethanol, 100 μg/ml mSCF, 50 ng/ml mTPO, 50 ng/ml mFlt3L, and 20 ng/ml mIL-3. Cells were transduced overnight with retroviruses from the pMIRWAY library[29], either in pools or individual members, on retronectin-coated plates (Takara) in the presence of 2 μg/ml polybrene. Following overnight infection, cells were resuspended and washed in PBS, and injected into the tail vein of recipient IgM^b-macroself mice that had been previously irradiated (on the same day) with two doses of 5.0 Gy separated by 3 h. Each recipient mouse received 2–5 $\times 10^6$ infected cells mixed with 0.5 $\times 10^6$ helper bone marrow cells from $CD45.1^+$ C57BL/6J mice. Eight weeks after reconstitution, recipient mice were sacrificed and the presence of B cells in the spleen was determined by cell surface staining with CD19 (6D5, Biolegend) and IgM (115-175-075, Jackson ImmunoResearch) antibodies and flow cytometry analysis. In pooled screening experiments, splenic B cells ($CD19^+$) and BM B cell precursors ($CD19^+IgM^-$) were purified using biotinylated antibodies and MACS magnetic beads following the manufacturer's instructions (Miltenyi Biotec). Genomic DNA was extracted from purified cells and subjected to miRNA barcode analysis as previously described[29].

MiRNA barcode detection

MiRNA barcodes were detected using a Luminex bead-based detection system as described previously[29]. Briefly, to create Luminex beads specific for miRNA barcodes, 5'amino-labeled bar-code detection oligonucleotides (IDT) were coupled to carboxylated MagPlex microspheres (Luminex), with each oligonucleotide coupled to beads with a unique color combination (referred to as region by the manufacturer). Coupling reactions were performed following the manufacturer's standard protocols. After coupling, beads of different colors were mixed together, washed with Tris-EDTA buffer (10 mM Tris, pH=8, 1 mM EDTA), and stored at 4 °C prior to being used in subsequent assays.

Hybridization to the MagPlex miRNA beadset was then performed. Beads were re-suspended in 1.5× TMAC buffer. A known amount of post-hybridization control oligonucleotides (/5Biosg/ CAACGGAATTCCTCACTAAACCCTGGACAGGCGAGGAATACAGTTTAACCGCGAA TTCCAGTA, 5Biosg/CAACGGAATTCCTCACTAAATGACTCTCAGCGA GCCTCAATGCTTTAACCGCGAATTCCAGTA, /5Biosg/CAACGGAATTCCT CACTAAACTGCGGGAGCCGATTTCATCTTTAACCGCGAATTCCAGTA) were spiked into the biotin-labeled barcode samples. Samples were then hybridized by denaturing at 95 °C for 10 min and incubating at 53 °C overnight. Following hybridization, beads were washed in 1× TMAC, incubated with 10 mg/ml Streptavidin-PE (Invitrogen) at 50 °C for 10

min, washed four times with 1× TMAC to remove free Streptavidin-PE, and re-suspended in a 45 μl final volume of TMAC. Raw barcode signals from each miRNA construct were acquired on a Luminex-FlexMap3D instrument. The acquired median fluorescence intensity values were then used in subsequent data analysis, and the relative signal of splenic B cells versus BM B cell precursors for each miRNA detected was calculated as previously described[29].

Stable cell line generation

WEHI-231 cells were grown in DMEM with 10% FBS 2 mmol/l L-glutamine and Pen/Strep, and 50 μM 2-mercaptoethanol. To generate the stable cell lines WEHI-control, WEHI-miR-148a, WEHI-miR-26a and WEHI-miR-182, the parental WEHI-231 cells were infected with the MSCV-control-GFP, MSCV-miR-148a–GFP, MSCV-miR-26a–GFP or MSCV-miR-182–GFP retroviruses in the presence of 8 μg/ml polybrene. Cells were expanded for 48 h and sorted by flow cytometry to purify the infected cells, which were grown for an additional 48 h, aliquoted, and stored in liquid nitrogen until use.

RNA hybridization

Total RNA was extracted from WEHI-control and WEHI-miR-148a stimulated with 2 μg/ml anti-IgM for 14 h or left unstimulated using TRIzol reagent following the manufacturer's instructions (Life Technologies). A DNA oligonucleotide antisense to mature miR-148a was used as probe for detecting miR-148a and U6 small nuclear RNA was used as an internal control for normalization. RNA hybridization results were acquired on a STORM 860 phophorimager.

TaqMan microRNA assays

Total RNA was extracted from cell samples using TRIzol reagent (Life Technologies), and reverse-transcribed using the TaqMan microRNA reverse transcription kit (Applied Biosystems) according to the manufacturer's protocol. TaqMan assays for miR-148a were performed with the Taqman universal master mix II (Applied Biosystems) in a CFX Connect real time PCR detection system (Biorad). miR-148a expression was normalized by U6 expression for each sample.

Apoptosis and proliferation assays

The Annexin V Apoptosis Detection Kit (eBioscience) and the Active Caspase 3 Apoptosis Kit (BD Pharmingen) were used for apoptosis assays. WEHI-control and WEHI-miR148a cells were stimulated with 2 μg/ml anti-IgM for the indicated amounts of time or left unstimulated, harvested, stained with both apoptosis kits following the manufacturer's protocols, and analyzed by flow cytometry for the markers annexin V and active caspase 3. For proliferation analysis, cells were labeled with the fluorescent dye Cell Trace Violet (Life Technologies) following the manufacturer's instructions, stimulated with 2 μg/ml anti-IgM for the indicated amounts of time or left unstimulated, and the dilution of the dye determined by flow cytometry.

B cell purification and stimulation

Mouse spleens were harvested, disaggregated into single-cell suspension, and follicular B cells were purified by negative selection using biotinylated CD9 (KMC8, BD Biosciences), CD43 (S7, BD Biosciences) and CD93 (AA4.1, eBioscience) antibodies and streptavidin-coated MACS beads (Miltenyi Biotec) according to the manufacturer's instructions. Purified follicular B cells samples were collected unstimulated or after stimulation for 48 h with 10 μg/ml anti-IgM (115-006-020, Jackson ImmunoResearch), 10 μg/ml LPS (Sigma) or both anti-IgM and LPS (10 μg/ml each).

RNA sequencing

Total RNA of WEHI-control and WEHI-miR148a cells stimulated with 2 μg/ml anti-IgM for 14 h or left unstimulated was purified using TRIzol reagent (Life Technologies). Total RNA of each sample (2 μg/sample) was submitted to the TSRI Next Generation Sequencing Core for deep sequencing. Total RNA was enriched for polyA-containing RNAs and deep sequencing of those samples was performed on a HiSeq 2000 (Illumina). Data analysis was performed with Pipeline Software (Casava v1.8.2) and Cutadapt. Alignment to the mouse genome was performed with mRNA-Seq TopHat v2.0.13 with Bowtie2, and the exon annotation retrieved with Partek. Total read counts for each gene was calculated and used to identify protein coding genes downregulated by miR-148a.

Quantitative RT-PCR

cDNA was synthesized by reverse transcription (Promega) of total RNA (1 μg). Quantitative reverse transcriptase PCR (qRT-PCR) reactions were performed using the Power SYBR Green PCR Master Mix System (Applied Biosystems) with specific primers for murine *Bcl2l11*, *Pten* and *Gadd45a* using *Actb* for normalization. The following primers were used for qRT-PCR analysis:

Bcl2l11 5′-GAGATACGGATTGCACAGGAG-3′ and 5′-CGGAAGATAAAGCGTAACAGTTG-3′,

Pten 5′-TGGGGAAGTAAGGACCAGAG-3′ and 5′-GGCAGACCACAAACTGAGGA-3′,

Gadd45a 5′-AGCAGAAGACCGAAAGGATG-3′ and 5′-GACTCCGAGCCTTGCTGA-3′,

Actb 5′-CTAAGGCCAACCGTGAAAG-3′ and 5′-ACCAGAGGCATACAGGGACA-3′.

Immunoblot

WEHI-control and WEHI-miR148a cells stimulated with 2 μg/ml anti-IgM for 14 h or left unstimulated were washed twice with PBS, and cell extracts were made by resuspending cell pellets in 1% NP-40 buffer containing 1% Nonidet P-40, 150 mM NaCl, 50 mM Tris-Cl (pH 8.0), 1 mM sodium orthovanadate, 1 mM DTT, and proteinase inhibitors (Thermo). 10 μg protein extract per sample was resolved in 10–12.5% gels by SDS-PAGE, transferred onto PVDF membranes, and detected with antibodies specific for murine Bim (Cell Signaling, 2933), Pten (Cell Signaling, 9559), and β-actin (Sigma clone AC-74). Images of the immunoblots were acquired on an Odyssey Fc machine (Li-cor).

Dual luciferase reporter assays

Murine miR-148a was cloned into the expression vector pCXN2, and 3′ UTR fragments of *Bcl2l11, Pten* and *Gadd45a* were cloned into the psiCHECK2 vector (Promega). The miR-148a binding sites in target gene 3'UTRs were mutated with the QuikChange Multi Site-Directed Mutagenesis Kit (Agilent Technologies). The resulting pCXN2 and psiCHECK2 plasmids were cotransfected into HEK293 cells using Fugene HD (Promega) according to the manufacturer's instructions. After 24 h cells were lysed and luciferase expression was measured using the Dual-luciferase assay system (Promega) following the manufacturer's protocol. The renilla luciferase (Rluc) was normalized by the firefly luciferase (Luc) signal, and the Rluc/Luc ratio was arbitrarily set as 1 for the control pCXN2 vector for each psiCHECK2 reporter.

Bone marrow transplantation

Donor bone marrow was collected from mice of indicated genotypes and used to reconstitute irradiated IgM^b-macroself mice. For each recipient mouse, 2–5 $\times 10^6$ donor bone marrow cells were mixed with 0.25 $\times 10^6$ helper bone marrow cells from $CD45.1^+$ C57BL/6J mice and injected intravenously into IgM^b-macroself mice that had had been previously irradiated (on the same day) with two doses of 5 Gy separated by 3 h.

MRL-lpr mice experiments

Donor MRL-lpr mice were treated with 5-fluorouracil for 4 days, and bone marrow cells were isolated and transduced with MSCV-control-GFP or MSCV-miR-148a-GFP. Transduced cells were used to reconstituted 6-week-old MRL-lpr recipient mice that had been previously irradiated (8.5 Gy). Each recipient mouse received 2–4 $\times 10^6$ infected bone marrow cells mixed with 0.5 $\times 10^6$ helper bone marrow cells from untreated MRL-lpr mice. Recipient mice were monitored periodically for disease onset and progression. Blood samples were collected at 8, 14 and 20 weeks post-reconstitution and serum was used for dsDNA-antibody analysis by ELISA as previously described[23]. Secondary lymphoid organs were collected at terminal analysis, weighed, and disaggregated to make single cell suspensions. The total cell number of the spleen, peripheral and mesenteric lymph nodes was determined by counting. $CD19^+B220^+$ B cells were analyzed by flow cytometry.

Statistical analysis

Data were analyzed using unpaired two-tailed Student's *t* test (*, $P<0.05$; **, $P<0.01$). The Kaplan-Meier curve was analyzed with a Log-rank test using Prism software.

Supplementary Material

Refer to Web version on PubMed Central for supplementary material.

ACKNOWLEDGEMENTS

We thank D. Kono for expert advice on analysis of lupus mice; L. Sherman for providing $Bcl2l11^{-/-}$ mice; members of the Xiao and Nemazee labs for advice and technical assistance; TSRI Flow Cytometry and Genomics Core Facilities for expert support. C.X. is a Pew Scholar in Biomedical Sciences. This study is supported by the PEW Charitable Trusts, Cancer Research Institute, Lupus Research Institute, and National Institute of Health (R01 AI089854 to C.X., R01 AI59714 to D.N. and RC4 AI092763 to C.X. and D.N.).

Accession code. GEO: RNA-seq dataset, GSE75809.

REFERENCES

1. Shlomchik MJ. Sites and stages of autoreactive B cell activation and regulation. Immunity. 2008; 28:18–28. [PubMed: 18199415]
2. Goodnow CC, Sprent J, Fazekas de St Groth B, Vinuesa CG. Cellular and genetic mechanisms of self tolerance and autoimmunity. Nature. 2005; 435:590–597. [PubMed: 15931211]
3. Nemazee D. Receptor editing in lymphocyte development and central tolerance. Nat Rev Immunol. 2006; 6:728–740. [PubMed: 16998507]
4. Tiller T, et al. Autoreactivity in human IgG+ memory B cells. Immunity. 2007; 26:205–213. [PubMed: 17306569]
5. Wardemann H, et al. Predominant autoantibody production by early human B cell precursors. Science. 2003; 301:1374–1377. [PubMed: 12920303]
6. Kinnunen T, et al. Specific peripheral B cell tolerance defects in patients with multiple sclerosis. J Clin Invest. 2013; 123:2737–2741. [PubMed: 23676463]
7. Samuels J, Ng YS, Coupillaud C, Paget D, Meffre E. Impaired early B cell tolerance in patients with rheumatoid arthritis. J Exp Med. 2005; 201:1659–1667. [PubMed: 15897279]
8. Yurasov S, et al. Defective B cell tolerance checkpoints in systemic lupus erythematosus. J Exp Med. 2005; 201:703–711. [PubMed: 15738055]
9. Bartel DP. MicroRNAs: target recognition and regulatory functions. Cell. 2009; 136:215–233. [PubMed: 19167326]
10. Kuchen S, et al. Regulation of microRNA expression and abundance during lymphopoiesis. Immunity. 2010; 32:828–839. [PubMed: 20605486]
11. Monticelli S, et al. MicroRNA profiling of the murine hematopoietic system. Genome Biol. 2005; 6:R71. [PubMed: 16086853]
12. O'Connell RM, Rao DS, Chaudhuri AA, Baltimore D. Physiological and pathological roles for microRNAs in the immune system. Nat Rev Immunol. 2010; 10:111–122. [PubMed: 20098459]
13. Xiao C, Rajewsky K. MicroRNA control in the immune system: basic principles. Cell. 2009; 136:26–36. [PubMed: 19135886]
14. Chauhan SK, Singh VV, Rai R, Rai M, Rai G. Differential microRNA profile and post-transcriptional regulation exist in systemic lupus erythematosus patients with distinct autoantibody specificities. J Clin Immunol. 2014; 34:491–503. [PubMed: 24659206]
15. Pan W, et al. MicroRNA-21 and microRNA-148a contribute to DNA hypomethylation in lupus CD4+ T cells by directly and indirectly targeting DNA methyltransferase 1. J Immunol. 2010; 184:6773–6781. [PubMed: 20483747]
16. Stagakis E, et al. Identification of novel microRNA signatures linked to human lupus disease activity and pathogenesis: miR-21 regulates aberrant T cell responses through regulation of PDCD4 expression. Annals of the rheumatic diseases. 2011; 70:1496–1506. [PubMed: 21602271]
17. Te JL, et al. Identification of unique microRNA signature associated with lupus nephritis. PLoS One. 2010; 5:e10344. [PubMed: 20485490]
18. Dai R, et al. Identification of a Common Lupus Disease-Associated microRNA Expression Pattern in Three Different Murine Models of Lupus. PLoS One. 2010; 5:e14302. [PubMed: 21170274]
19. Lindberg RL, Hoffmann F, Mehling M, Kuhle J, Kappos L. Altered expression of miR-17-5p in CD4+ lymphocytes of relapsing-remitting multiple sclerosis patients. Eur J Immunol. 2010; 40:888–898. [PubMed: 20148420]
20. Qin HH, et al. The expression and significance of miR-17-92 cluster miRs in CD4+ T cells from patients with systemic lupus erythematosus. Clin Exp Rheumatol. 2013; 31:472–473. [PubMed: 23432993]
21. Simpson LJ, et al. A microRNA upregulated in asthma airway T cells promotes TH2 cytokine production. Nat Immunol. 2014; 15:1162–1170. [PubMed: 25362490]
22. Kang SG, et al. MicroRNAs of the miR-17 approximately 92 family are critical regulators of T(FH) differentiation. Nat Immunol. 2013; 14:849–857. [PubMed: 23812097]

23. Xiao C, et al. Lymphoproliferative disease and autoimmunity in mice with increased miR-17-92 expression in lymphocytes. Nat Immunol. 2008; 9:405–414. [PubMed: 18327259]
24. Luo X, et al. A functional variant in microRNA-146a promoter modulates its expression and confers disease risk for systemic lupus erythematosus. PLoS genetics. 2011; 7:e1002128. [PubMed: 21738483]
25. Tang Y, et al. MicroRNA-146A contributes to abnormal activation of the type I interferon pathway in human lupus by targeting the key signaling proteins. Arthritis and rheumatism. 2009; 60:1065–1075. [PubMed: 19333922]
26. Boldin MP, et al. miR-146a is a significant brake on autoimmunity, myeloproliferation, and cancer in mice. J Exp Med. 2011; 208:1189–1201. [PubMed: 21555486]
27. Hu R, et al. miR-155 promotes T follicular helper cell accumulation during chronic, low-grade inflammation. Immunity. 2014; 41:605–619. [PubMed: 25367574]
28. Lu LF, et al. Function of miR-146a in controlling Treg cell-mediated regulation of Th1 responses. Cell. 2010; 142:914–929. [PubMed: 20850013]
29. Adams BD, et al. An in vivo functional screen uncovers miR-150-mediated regulation of hematopoietic injury response. Cell Rep. 2012; 2:1048–1060. [PubMed: 23084747]
30. Duong BH, et al. Negative selection by IgM superantigen defines a B cell central tolerance compartment and reveals mutations allowing escape. J Immunol. 2011; 187:5596–5605. [PubMed: 22043016]
31. Lu R, Neff NF, Quake SR, Weissman IL. Tracking single hematopoietic stem cells in vivo using high-throughput sequencing in conjunction with viral genetic barcoding. Nat Biotechnol. 2011; 29:928–933. [PubMed: 21964413]
32. Haftmann C, et al. miR-148a is upregulated by Twist1 and T-bet and promotes Th1-cell survival by regulating the proapoptotic gene Bim. Eur J Immunol. 2015; 45:1192–1205. [PubMed: 25486906]
33. Dai R, et al. Sex differences in the expression of lupus-associated miRNAs in splenocytes from lupus-prone NZB/WF1 mice. Biol Sex Differ. 2013; 4:19. [PubMed: 24175965]
34. Scott DW, Livnat D, Pennell CA, Keng P. Lymphoma models for B cell activation and tolerance. III. Cell cycle dependence for negative signalling of WEHI-231 B lymphoma cells by anti-mu. J Exp Med. 1986; 164:156–164. [PubMed: 3487612]
35. Scott DW, et al. Lymphoma models for B-cell activation and tolerance. II. Growth inhibition by anti-mu of WEHI-231 and the selection and properties of resistant mutants. Cell. Immunol. 1985; 93:124–131. [PubMed: 3922631]
36. Bouillet P, et al. Proapoptotic Bcl-2 relative Bim required for certain apoptotic responses, leukocyte homeostasis, and to preclude autoimmunity. Science. 1999; 286:1735–1738. [PubMed: 10576740]
37. Erickson SL, et al. Decreased sensitivity to tumour-necrosis factor but normal T-cell development in TNF receptor-2-deficient mice. Nature. 1994; 372:560–563. [PubMed: 7990930]
38. Lesche R, et al. Cre/loxP-mediated inactivation of the murine Pten tumor suppressor gene. Genesis. 2002; 32:148–149. [PubMed: 11857804]
39. Rickert RC, Roes J, Rajewsky K. B lymphocyte-specific, Cre-mediated mutagenesis in mice. Nucleic Acids Res. 1997; 25:1317–1318. [PubMed: 9092650]
40. Salvador JM, et al. Mice lacking the p53-effector gene Gadd45a develop a lupus-like syndrome. Immunity. 2002; 16:499–508. [PubMed: 11970874]
41. Enders A, et al. Loss of the pro-apoptotic BH3-only Bcl-2 family member Bim inhibits BCR stimulation-induced apoptosis and deletion of autoreactive B cells. J Exp Med. 2003; 198:1119–1126. [PubMed: 14517273]
42. Cheng S, et al. BCR-mediated apoptosis associated with negative selection of immature B cells is selectively dependent on Pten. Cell Res. 2009; 19:196–207. [PubMed: 18781138]
43. Andrews BS, et al. Spontaneous murine lupus-like syndromes. Clinical and immunopathological manifestations in several strains. J Exp Med. 1978; 148:1198–1215. [PubMed: 309911]
44. Shen N, Liang D, Tang Y, de Vries N, Tak PP. MicroRNAs--novel regulators of systemic lupus erythematosus pathogenesis. Nat. Rev. Rheumatol. 2012; 8:701–709. [PubMed: 23070646]
45. Di Cristofano A, et al. Impaired Fas response and autoimmunity in Pten+/− mice. Science. 1999; 285:2122–2125. [PubMed: 10497129]

46. Oliver PM, Vass T, Kappler J, Marrack P. Loss of the proapoptotic protein, Bim, breaks B cell anergy. J Exp Med. 2006; 203:731–741. [PubMed: 16520387]

47. Browne CD, Del Nagro CJ, Cato MH, Dengler HS, Rickert RC. Suppression of phosphatidylinositol 3,4,5-trisphosphate production is a key determinant of B cell anergy. Immunity. 2009; 31:749–760. [PubMed: 19896393]

48. Salvador JM, Brown-Clay JD, Fornace AJ Jr. Gadd45 in stress signaling, cell cycle control, and apoptosis. Adv Exp Med Biol. 2013; 793:1–19. [PubMed: 24104470]

49. Salvador JM, Mittelstadt PR, Belova GI, Fornace AJ Jr, Ashwell JD. The autoimmune suppressor Gadd45alpha inhibits the T cell alternative p38 activation pathway. Nat Immunol. 2005; 6:396–402. [PubMed: 15735649]

50. Tong T, et al. Gadd45a expression induces Bim dissociation from the cytoskeleton and translocation to mitochondria. Mol Cell Biol. 2005; 25:4488–4500. [PubMed: 15899854]

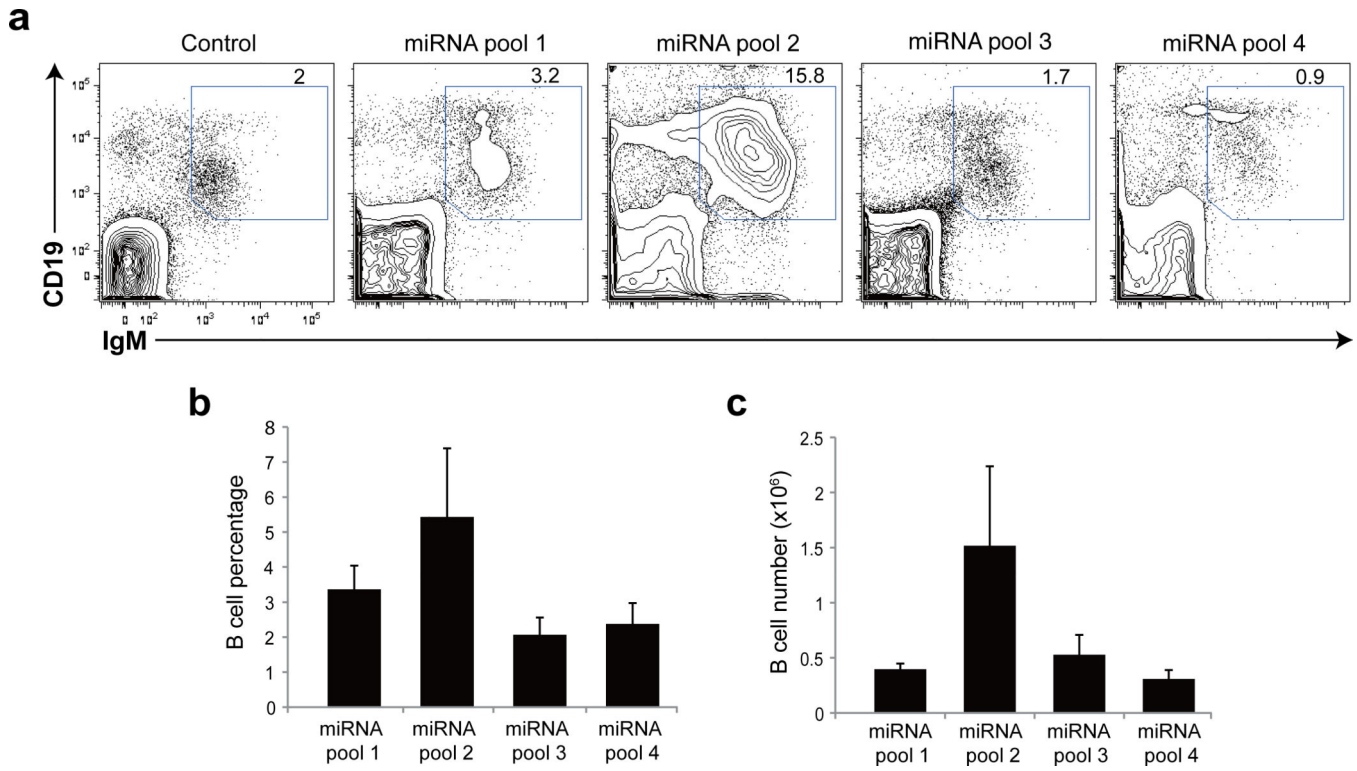

Figure 1. ***In vivo*** **functional screen of miRNAs regulating B cell tolerance**

(**a**) Representative FACS plots showing splenic B cells ($CD19^+IgM^+$) of IgM^b-macroself mice reconstituted with miRNA-transduced HSPCs at terminal analysis. The control group received donor cells transduced with retroviruses encoding no miRNA. (**b,c**) Percentages of B cells in total splenocytes (**b**) and numbers of splenic B cells (**c**) in mice analyzed in a. Data are pooled from four individual experiments (**a–c**; mean ± s.e.m. in **b,c**): n=5 in control, miRNA-pool 3 and miRNA pool 4 groups and n=6 in miRNA pool 1 and miRNA pool 2 groups.

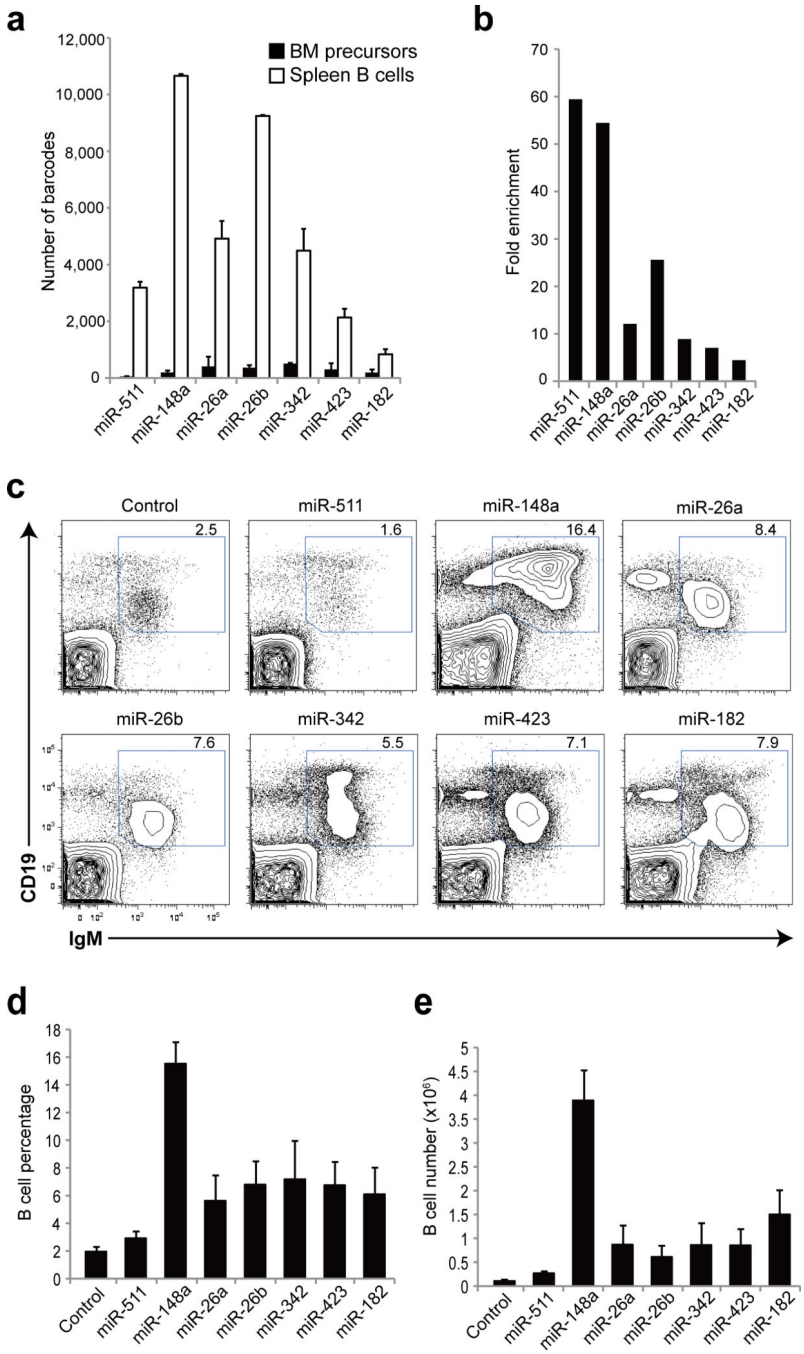

Figure 2. miR-148a promotes B cell escape from the central tolerance checkpoint

(**a,b**) Barcode identification of the miRNA screen showing number of barcodes (**a**) and fold enrichment (**b**) of the top hit miRNAs in splenic B cells as compared to bone marrow B cell precursors. (**c**) Representative FACS plots showing splenic B cells ($CD19^+IgM^+$) in IgM^b-macroself recipient mice reconstituted with HSPCs transduced with the individual top hits miRNAs at terminal analysis. (**d,e**) Percentages (**d**) and numbers (**e**) of splenic B cells in mice analyzed in c. Data are representative of three independent experiments (**a,b**; mean ± s.d. of technical triplicates in **a**), or pooled from nine individual experiments (**c–e**; mean ±

s.e.m.): n=5 mice in control, miR-511 and miR-423, n=6 mice in miR-148a and miR-26a, n=4 mice in miR-26b and miR-342, and n=8 mice in miR-182 group.

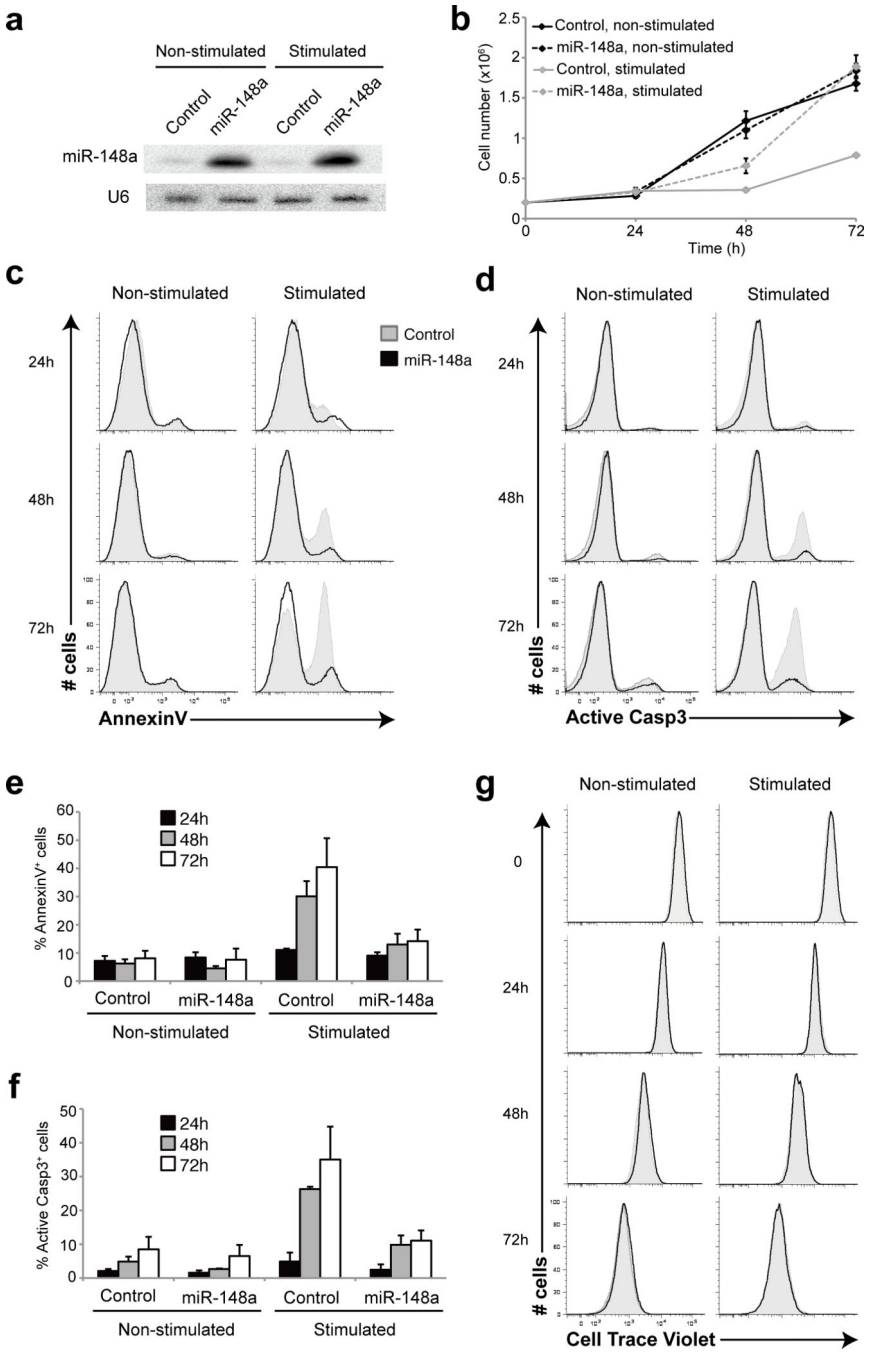

Figure 3. miR-148a protects immature B cells from apoptosis induced by BCR engagement

(**a**) RNA hybridization analysis showing miR-148a expression in WEHI-control and WEHI-miR-148a cells stimulated with 2μg/ml anti-IgM for 14h or left unstimulated. U6 was used as an internal control. (**b**) The growth curves of WEHI-control and WEHI-miR-148a cells in non-stimulated and stimulated (2μg/ml anti-IgM) conditions. (**c,d**) Representative FACS histograms showing apoptotic cells by Annexin V (**c**) and active caspase 3 (**d**) analysis of non-stimulated and stimulated (2μg/ml anti-IgM) WEHI-control and WEHI-miR-148a at the indicated times. (**e,f**) Percentages of Annexin V- (**e**) and active Caspase 3- (**f**) positive cells

in two independent experiments. (**g**) Representative FACS histograms showing cell proliferation in WEHI-control and WEHI-miR-148a cells labeled with the fluorescent dye Cell Trace Violet, stimulated with 2μg/ml anti-IgM or left unstimulated, and analyzed at the indicated times for fluorescence dilution. Dead cells were excluded from the histogram analysis. Data are representative of two independent experiments (**a–d,g**; mean ± s.d. in **b**) or are pooled from two independent experiments (**e,f**; mean ± s.d.).

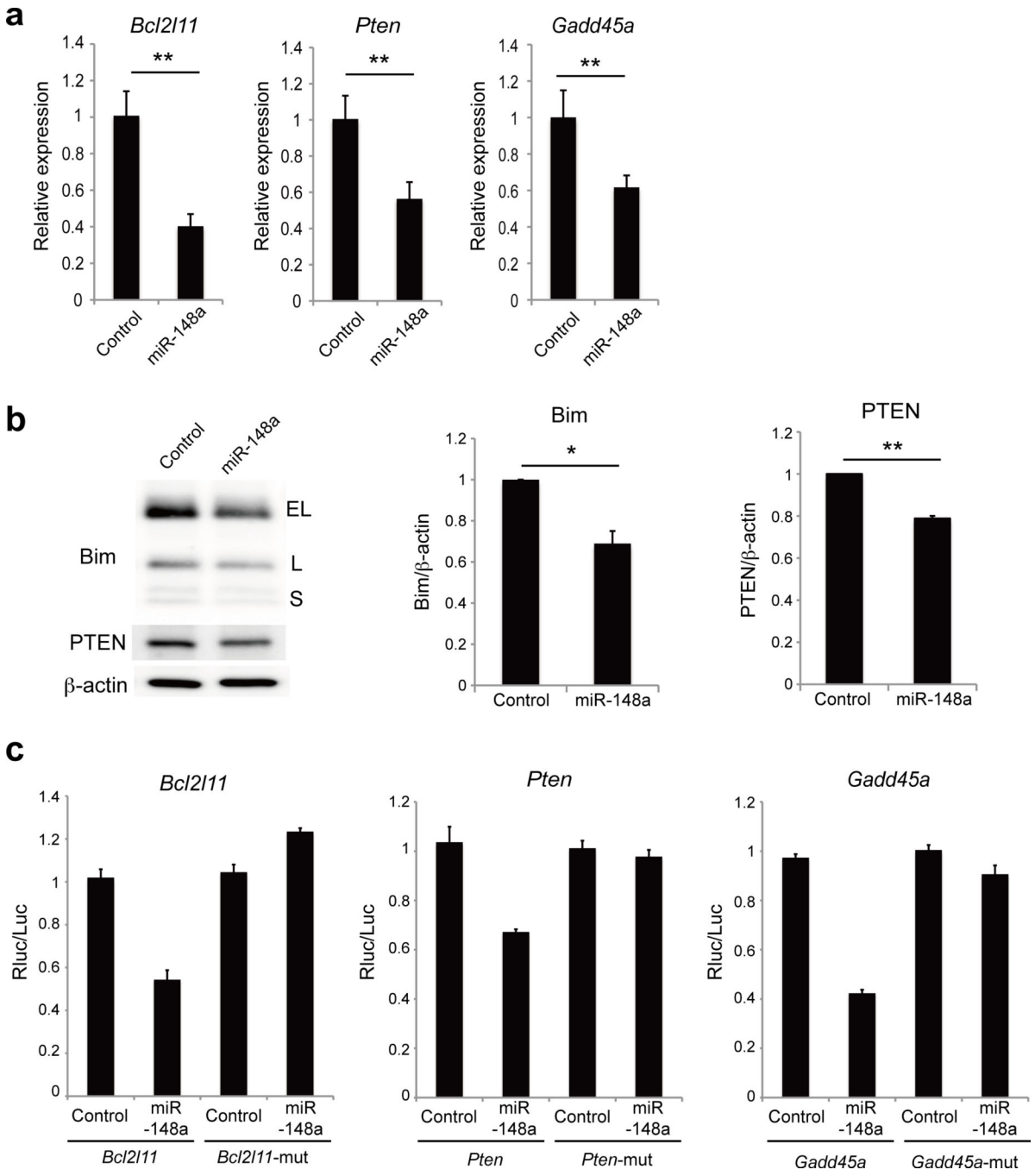

Figure 4. miR-148a suppresses the expression of Bim, PTEN, and Gadd45a

(**a**) qRT-PCR analysis showing target genes *Bcl2l11*, *Pten* and *Gadd45a* mRNA expression in stimulated (2μg/ml anti-IgM) WEHI-control and WEHI-miR-148a for 14 h. (**b**) Immunoblot analysis showing target genes Bim (isoforms EL, L and S) and PTEN expression in the same conditions as in **a**. The target gene protein/β-actin ratio was arbitrarily set as 1. (**c**) Dual luciferase reporter assays showing direct interaction of miR-148a with its cognate binding sites in the 3'UTR regions of *Bcl2l11*, *Pten* and *Gadd45a*. *Bcl2l11*-mut, *Pten*-mut and *Gadd45a*-mut refer to constructs with mutated cognate

binding sites for miR-148a. The renilla luciferase (Rluc) signal regulated by the target gene ´s 3'UTR was normalized by the firefly luciferase (Luc). The Rluc/Luc ratio was arbitrarily set as 1 for the control pCXN2 plasmid in each experiment. Data are pooled from two individual experiments (**a,b**; mean ± s.d.) or representative of two independent experiments (**c**; mean ± s.d. of technical triplicates). Statistical analysis was performed with a two-tailed Student's T test. *P<0.05, ** P<0.01.

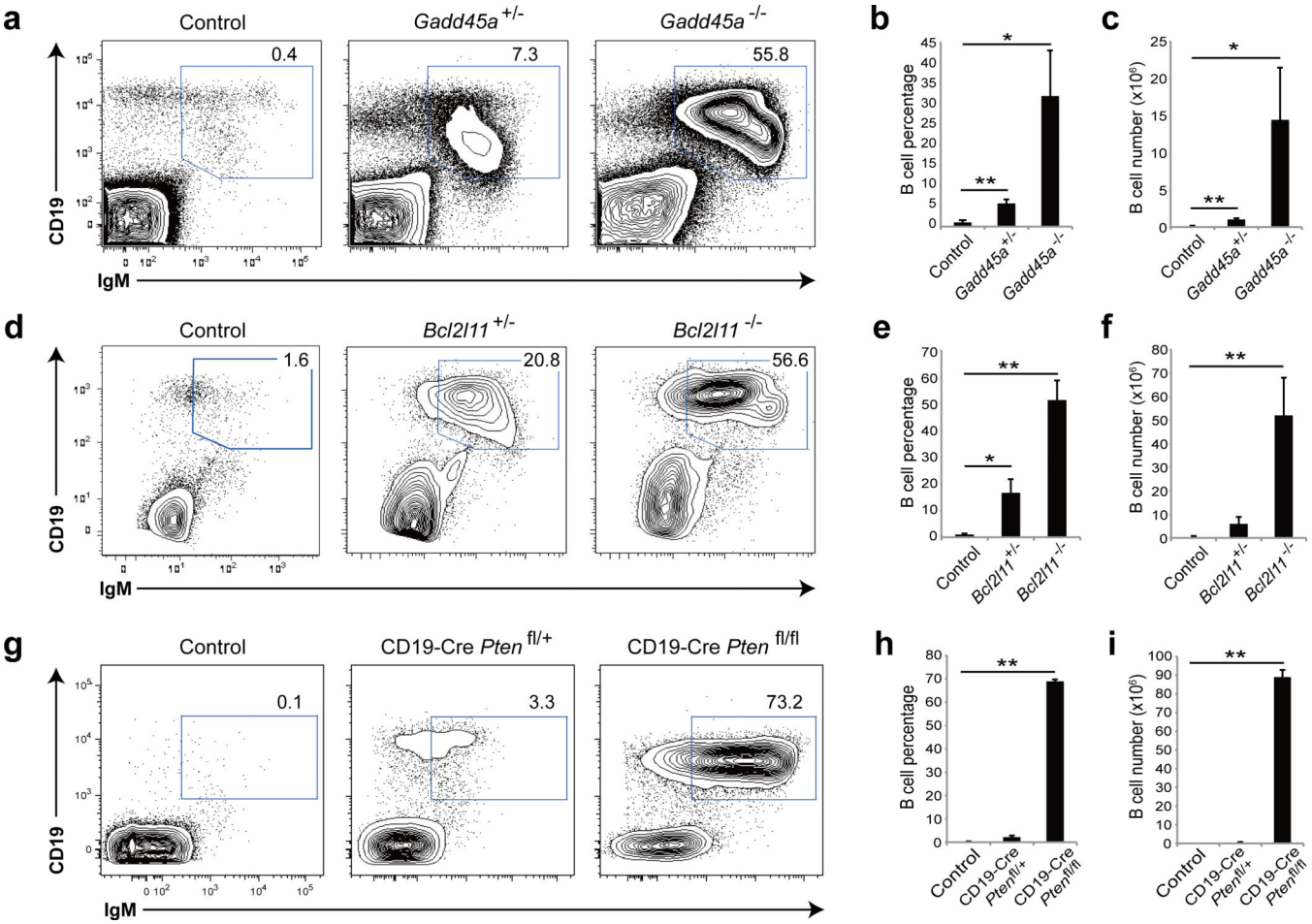

Figure 5. Deletion of the *Gadd45a*, *Bcl2l11* and *Pten* genes impairs B cell tolerance

(**a, d and g**) Representative FACS plots showing splenic B cells ($CD19^+IgM^+$) of IgM^b-macroself recipient mice reconstituted with bone marrow cells of the indicated genotypes at terminal analysis. (**b, c, e, f, h, i**) Percentages (**b, e, h**) and numbers (**c, f, i**) of splenic B cells in mice analyzed in **a, d** and **g**. Data are pooled from five individual experiments (**a,b**; mean ± s.e.m. in **b**) or four individual experiments (**c**; mean ± s.e.m.) or three individual experiments (**d–i**; mean ± s.e.m. in **e, f, h, i**): n=5, 6 and 8 mice for control, *Gadd45a*$^{+/-}$ and *Gadd45a*$^{-/-}$ respectively in **a,b**, n=5, 6 and 5 mice in control, *Gadd45a*$^{+/-}$ and *Gadd45a*$^{-/-}$ respectively in **c**, n=7, 11 and 6 mice in control, *Bcl2l11*$^{+/-}$ and *Bcl2l11*$^{-/-}$ respectively in **d–f**, and n= 3, 5 and 6 mice in control, *Cd19*-Cre *Pten*$^{fl/+}$ and *Cd19*-Cre *Pten*$^{fl/fl}$ groups respectively in **g–i**. Statistical analysis was performed with a two-tailed Student's T test. *P<0.05, ** P<0.01.

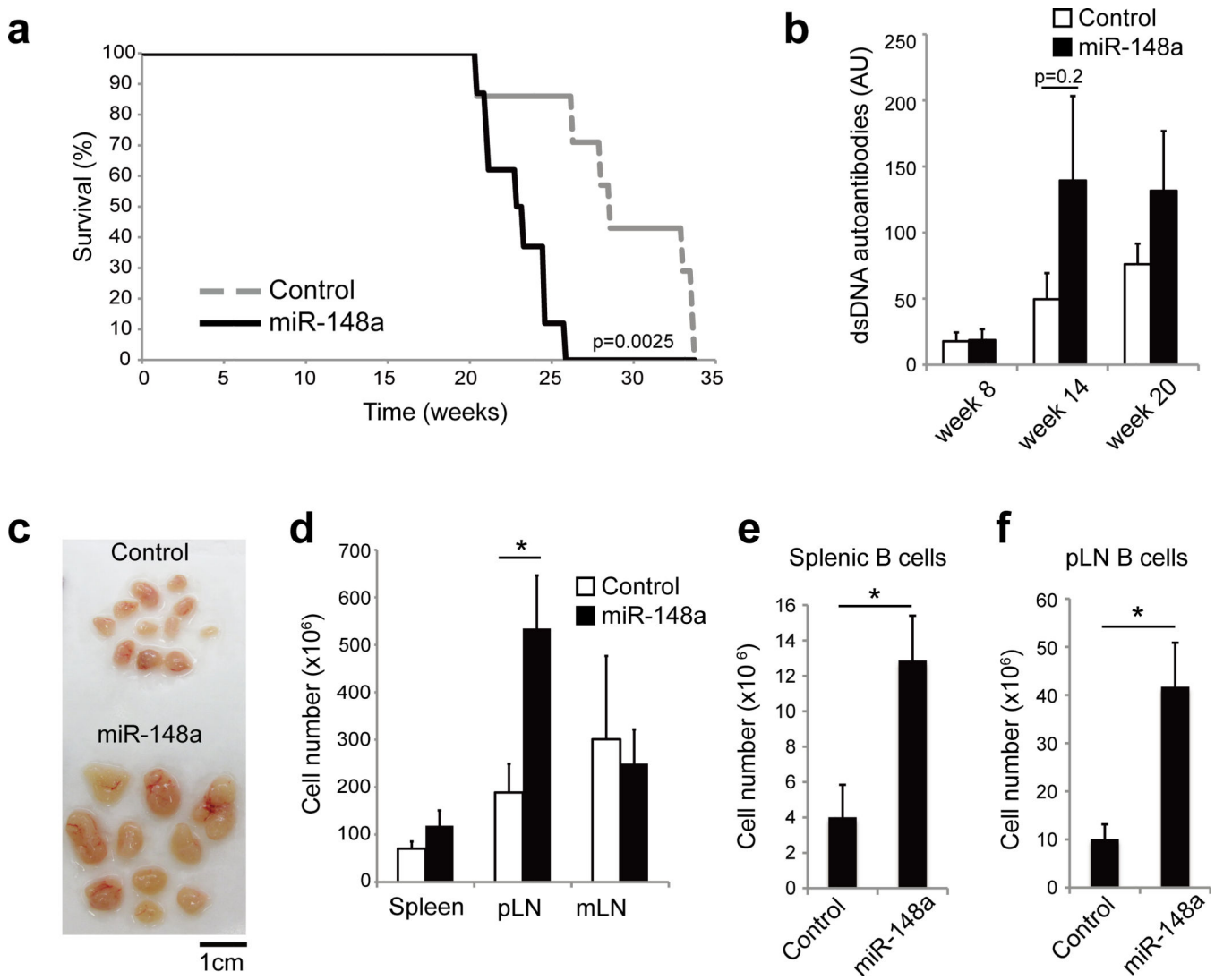

Figure 6. Increased miR-148a expression facilitates the development of lethal autoimmunity

(**a**) Kaplan-Meier curve showing survival analysis of MLR-lpr mice reconstituted with control or miR-148a-transduced HSPCs from MRL-lpr mice previously treated with 5-fluorouracil. n=7 mice for control and n=8 mice for miR-148a group. Statistical analysis was performed with a Log-rank test. (**b**) ELISA quantification of serum levels of anti-dsDNA autoantibodies of the mice in a at the indicated times. (**c**) Representative images of peripheral lymph nodes (pLNs) at terminal analysis. (**d**) Total cell numbers in the spleen, peripheral lymph nodes (pLN) and mesenteric lymph nodes (mLN) at terminal analysis. (**e,f**) Total numbers of B cells ($CD19^+B220^+$) in the spleen (**e**) and pLN (**f**) at terminal analysis. Data were pooled from two independent experiments (**a–f**; mean ± s.e.m. in **b, d, e** and **f**). n=6 mice for control and n=8 mice for miR-148a group in **c–f**. Statistical analysis was performed with a two-tailed Student's T test. *P<0.05.

Table 1

miRNA retroviral pools.

miRNA pool 1	Let-7a	miR-103	miR-33
miR-93	Let-7c	miR-423	miR-147
miR-125a	Let-7g	miR-107	miR-421
miR-125b	Let-7i	miR-511	miR-219-1
miR-21	Let-7d	miR-101	miR-330
miR-23a	Let-7b	miR-128b	miR-362
miR-23b	Let-7e	miR-185	miR-122a
miR-24	miR-1	miR-192	miR-328
miR-27a		miR-148a	
miR-27b	**miRNA pool 2**	miR-98	**miRNA pool 4**
miR-181a	miR-223		miR-339
miR-181b	miR-10a	**miRNA pool 3**	miR-455
miR-181c	miR-182	miR-423	miR-193b
miR-181d	miR-96	miR-199a-1	miR-324
miR-142	miR-183	miR-7-1	miR-500
miR-15a	miR-31	miR-130b	miR-365-1
miR-15b	miR-140	miR-130a	miR-194-2
miR-16	miR-191	miR-186	miR-598
miR-29a	miR-378	miR-374	miR-127
miR-29b	miR-221	miR-345	miR-499
miR-29c	miR-26a	miR-503	miR-326
miR-146a	miR-26b	miR-139	miR-504
miR-155	miR-342	miR-501	miR-451
miR-150	miR-22	miR-151	miR-671
miR-30a	miR-425	miR-652	miR-188
miR-30b	miR-34a	miR-872	miR-143
miR-30c	miR-34c	miR-331	miR-138
miR-30d	miR-99a	miR-28	miR-211
miR-30e	miR-99b	miR-361	miR-184
Let-7f	miR-200c	miR-206	miR-32